Metabolomics (2012) 8:624–633
DOI 10.1007/s11306-011-0353-9

ORIGINAL ARTICLE

Non-targeted metabolite profiling in activated macrophage secretion

Masahiro Sugimoto · Hiroshi Sakagami · Yoshiko Yokote · Hiromi Onuma · Miku Kaneko · Masayo Mori · Yasuko Sakaguchi · Tomoyoshi Soga · Masaru Tomita

Received: 29 March 2011 / Accepted: 9 August 2011 / Published online: 24 August 2011

Abstract Periodontal diseases are inflammatory infectious diseases that affect the periodontal tissue. Macrophages play a central role in inflammatory conditions, leading to the destruction of tissues. Identifying the signaling molecules secreted by macrophages would be valuable to the study of these diseases. Here, we present non-targeted analysis using capillary electrophoresis time-of-flight mass spectrometry (CE-TOFMS) for the profiling of extracellular metabolites released during macrophage activation. Lipopolysaccharide (LPS)-induced activation of a mouse macrophage-like cell line RAW264.7 was used as a model system. Cells were treated without (control) or with LPS for 22 h and, after washing, were incubated for 1 h in phosphate-buffered saline. The accumulation of metabolites in the culture supernatant was monitored. LPS treatment significantly enhanced the accumulation of prostaglandins, tumor necrosis factor-α, nitric oxide and citrulline in the culture medium. RAW264.7 cells produced 46 metabolites and 66% of these showed significant changes ($P < 0.05$) following cell activation. In particular, the production of leucine, hypoxanthine, choline, putrecine, N_8-acetylspermidine, succinate, itaconate, and 4-methyl-2-oxopentanoate was significantly increased by cell activation ($P < 0.001$). Significantly elevated production of lactate and glycine was also observed. Here, we present the first catalog of the up and down-regulation of the various metabolites secreted by macrophages following inflammatory activation.

Keywords Macrophage activation · Lipopolysaccharide · RAW264.7 cells · Capillary electrophoresis-mass spectrometry

1 Introduction

Periodontal disease and its milder form, gingivitis, affects 50–90% of adults worldwide, depending on the precise definition of the disease (Pihlstrom et al. 2005). The disease results in the destruction of periodontal tissues and the supporting dental structure, and is associated with systemic diseases such as diabetes, cancer, cardiovascular disease, and preterm birth (Meyer et al. 2008). Periodontal diseases are caused by complex interactions between the host tissue and bacteria at the junctional and crevicular epithelia, and is mainly mediated by the host's response to bacteria (Van Dyke and Serhan 2003).

Neutrophils and macrophages play important roles in the innate inflammatory response during the progression of periodontal disease, with sequential events being triggered by lipopolysaccharide (LPS) from gram-negative bacteria at the tooth root surface. Polymorphonuclear leukocytes are

M. Sugimoto and H. Sakagami contributed equally to this work.

M. Sugimoto (✉) · H. Onuma · M. Kaneko · M. Mori · Y. Sakaguchi · T. Soga · M. Tomita
Institute for Advanced Biosciences, Keio University, Tsuruoka, Yamagata 997-0017, Japan
e-mail: msugi@sfc.keio.ac.jp

M. Sugimoto · T. Soga · M. Tomita
Systems Biology Program, Graduate School of Media and Governance, Keio University, Fujisawa, Kanagawa 252-8520, Japan

H. Sakagami
Divisions of Pharmacology, Meikai University School of Dentistry, Sakado, Saitama 350-0283, Japan

Y. Yokote
Faculty of Science, Josai University, Sakado, Saitama 350-0295, Japan

recruited to the site, and monocytes and activated macrophages respond to endotoxin by releasing various cytokines and interleukin-1β, which stimulates further tissue destruction (Giannobile et al. 2009). Therefore, understanding the biochemical cascades induced by macrophages is important for the diagnosis and treatment of periodontal diseases.

Macrophages perform a multitude of functions essential for tissue remodeling and the immune response, and produce a wide array of pro-inflammatory cytokines, growth factors, lysozymes, proteases, complement components, coagulation factors and prostaglandins upon stimulation with LPS or hypoxic stress (Bingle et al. 2002). A mouse macrophage-like cell line (RAW264.7) (Ralph and Nakoinz 1977) has been used by many investigators in experiments designed to elucidate the signal transduction events during macrophage activation. Using this cell line, we have previously profiled amino acid release and found that the extracellular levels of glycine were significantly elevated during LPS-induced activation (Nishiyama et al. 2010). Glycine is the most abundant amino acid found in saliva (Nakamura et al. 2010) and salivary glycine levels are significantly elevated in elderly persons regardless of gender (Tanaka et al. 2010). This suggests that activated macrophages may be involved in age-related changes to salivary composition. Elevated levels of glycine in the saliva of elderly persons may aggravate periodontitis by stimulating the production of prostaglandin E_2 and cyclooxygenase-2 (COX-2) protein by interleukin-1β-stimulated human gingival fibroblast cells (Rausch-Fan et al. 2005). However, the importance of changes in glycine levels relative to other intracellular metabolite changes induced in activated macrophages remains unclear.

Metabolomics, the simultaneous quantification of all intercellular or intracellular metabolites, has become a powerful new tool that can provide insight into cellular functions (Soga et al. 2003). Several metabolites have been identified as endogenous chemical mediators that orchestrate the host's response in periodontal diseases. These metabolites include lipid-derived mediators, key inflammation signaling molecules (Van Dyke and Serhan 2003), and adenosine and inosine (Cronstein et al. 1999a, b), which are upregulated by cells in response to stress. Although the metabolite profiles of individual pathways, including lipid (Van Dyke and Serhan 2003), amino acid (Li et al. 2007) and carbohydrate (Rodriguez-Prados et al. 2010) metabolites, have been revealed, a broad understanding of these metabolomic profiles is necessary to determine the pathogenic mechanisms involved in innate macrophage inflammation in periodontal diseases.

In this study, we present the first comprehensive metabolomic analysis of the culture supernatants of unstimulated and stimulated macrophage cells to identify the metabolites secreted from macrophages at inflammatory sites such as periodontal tissues during periodontal disease. To profile a wide range of metabolites, non-targeted analyses of the extracellular environment of RAW264.7 cells treated without and with LPS were conducted using capillary electrophoresis time-of-flight mass spectrometry (CE-TOFMS) (Soga et al. 2006).

2 Materials and methods

2.1 Materials

Dulbecco's modified Eagle medium (DMEM) was purchased from GIBCO BRL (Grand Island, NY, USA), fetal bovine serum (FBS) was from JRH Biosciences (Lenexa, KS, USA) and LPS from *E. coli*, Serotype 0111:B4 was purchased from Sigma (St. Louis, MO, USA). Ophthalmate was purchased from Bachem AG (Bubendorf, Switzerland). Acetohydroxamate and azetidine-2-carboxylate were purchased from Chem Service (West Chester, PA, USA). Glucose 1-phosphate and 5-aminovalerate were purchased from Fluka (Buchs, Switzerland). Betaine was purchased from Tokyo Chemical Industry (Tokyo, Japan). All other compounds were purchased from Sigma-Aldrich (St. Louis, MO, USA) or Wako (Osaka, Japan).

2.2 Cell culture

Mouse macrophage-like RAW264.7 cells (purchased from Dainippon Sumitomo Pharma, Osaka, Japan) were cultured at 37°C in DMEM supplemented with 10% FBS under a humidified 5% CO_2 atmosphere.

2.3 LPS activation

Cells (8×10^5 cells/ml, 2 ml) were inoculated on a six-well plate (Becton–Dickinson, Labware, NJ, USA) and incubated at 37°C for 4 h for the cells to completely adhere to the plate. The medium was changed with fresh medium and the cells were then incubated for 22 h without (LPS−) or with 100 ng/ml LPS (LPS+). The experiment was carried out in triplicate. The cells were washed twice with phosphate-buffered saline without calcium or magnesium (PBS−), and then incubated in 1 mL of PBS−. An aliquot (0.5 ml) was removed immediately from each well to provide samples to analyze the initial metabolite mixture, and the cells were then incubated for 60 min at 37°C with the remaining 0.5 ml of PBS− in a 5% CO_2 incubator. All samples were centrifuged ($10{,}000 \times g$, 60 min) through a 3-kDa cutoff filter (Pall Corporation, NY, USA) to remove macromolecules, and the filtrates were assayed to detect nitric oxide (NO), tumor necrosis factor-α (TNF-α), amino acids and other cellular metabolites as described below.

A short incubation time (60 min) was used to minimize cell damage during incubation in PBS−. After incubation, the number of viable cells, which were not stained with 0.15% trypan blue in PBS−, was counted using a hemocytometer under a light microscope. The production rate for each compound was determined by subtracting the initial value from the value obtained after 60 min incubation, and expressed as nmol/10^6 cells/h.

2.4 NO assay

Since NO is a highly unstable compound, NO present in the culture medium was detected directly, without centrifugation, using the Griess method (Takahashi et al. 2008).

2.5 TNF-α assays

The culture supernatants were assayed using an ELISA kit (R&D Systems Inc, Minneapolis, MN, USA) to measure the concentration of TNF-α. The assay was performed according to the manufacturer's instructions.

2.6 Sample preparation for CE-TOFMS

To 100 μl of the extracellular-dissolved samples, 400 μl of methanol containing internal standards (50 μmol/l each of methionine sulfone, 2-[*N*-morpholino]-ethanesulfonic acid, and D-camphor-10-sulfonic acid) was added. The homogenate was then mixed with Milli-Q water and chloroform at a volume ratio of 5:2:5, and the mixture was centrifuged at 20,400×*g*, for 15 min at 4°C. The aqueous layer was filtered to remove macromolecules by centrifugation through a 5-kDa cutoff filter (Millipore) at 9,100×*g* for 2.5 h at 4°C. The filtrate (300 μl) was concentrated by centrifugation and dissolved in 50 μl of Milli-Q water containing reference compounds (200 μmol/l each of 3-aminopyrrolidine and trimesate) immediately before CE-TOFMS analysis.

2.7 Instrumental parameters for CE-TOFMS

The instrumentation and measurement conditions used for CE-TOFMS are described elsewhere (Sugimoto et al. 2010a; Soga et al. 2006, 2009). Cation analysis was performed using an Agilent CE capillary electrophoresis system, an Agilent G6220A LC/MSD TOF system, an Agilent 1100 series isocratic HPLC pump, a G1603A Agilent CE-MS adapter kit, and a G1607A Agilent CE-ESI-MS sprayer kit (Agilent Technologies, Waldbronn, Germany). Anion analysis was performed using an Agilent CE capillary electrophoresis system, an Agilent G6210A LC/MSD TOF system, an Agilent 1200 series isocratic HPLC pump, a G1603A Agilent CE-MS adapter kit and a G1607A Agilent CE-electrospray ionization (ESI) source-MS sprayer kit (Agilent Technologies). For both the cation and anion analyses, the CE-MS adapter kit includes a capillary cassette that enables thermostatic control of the capillary. The CE-ESIMS sprayer kit simplifies coupling of the CE system with the MS systems and is equipped with an electrospray source. For system control and data acquisition, we used G2201AA Agilent ChemStation software for CE and Agilent MassHunter software for TOF-MS. For anion analysis, the original Agilent SST316Ti stainless steel ESI needle was replaced with a SST316Ti stainless steel and platinum needle, which was passivated using 1% formic acid and 20% isopropanol aqueous solution at 80°C for 30 min.

For cationic metabolite analysis using CE-TOFMS (Soga et al. 2006), the samples were separated in fused silica capillaries (50 μm i.d. × 100 cm total length) filled with 1 mol/l formic acid as the reference electrolyte. Sample solutions were injected at 50 mbar for 3 s and a voltage of 30 kV was applied. The capillary temperature was maintained at 20°C and the temperature of the sample tray was kept below 5°C. The sheath liquid, composed of methanol/water (50% v/v) and 0.1 μmol/l hexakis (2,2-difluoroethoxy) phosphazene (Hexakis), was delivered at 10 μl/min. ESI-TOF-MS was conducted in the positive ion mode. The capillary voltage was set at 4 kV and the flow rate of nitrogen gas (heater temperature = 300°C) was set at 10 psig. In TOF-MS, the fragmentor, skimmer and OCT RF voltages were set at 75, 50 and 125 V, respectively. Automatic recalibration of each acquired spectrum was performed using reference masses of reference standards {[^{13}C isotopic ion of protonated methanol dimer $(2MeOH + H)]^+$, *m/z* 66.063061) and ([protonated Hexakis $(M + H)]^+$, *m/z* 622.02896}. Mass spectra were acquired at the rate of 1.5 cycles/s over a *m/z* range of 50–1,000.

For anionic metabolite analysis using CE-TOFMS (Soga et al. 2009), a commercially available COSMO(+) capillary (50 μm i.d. × 110 cm, Nacalai Tesque, Kyoto, Japan), chemically coated with a cationic polymer, was used for separation. A 50-mmol/l ammonium acetate solution (pH 8.5) was used as the electrolyte to achieve separation. Before the first use, a new capillary was flushed successively for 10 min each with the running electrolyte (pH 8.5), 50 mmol/l acetic acid (pH 3.4), and then the electrolyte again. Before each injection, the capillary was equilibrated for 2 min by flushing with 50 mM acetic acid (pH 3.4) and then for 5 min by flushing with the running electrolyte. A sample solution (30 nl) was injected at 50 mbar for 30 s, and a voltage of −30 kV was applied. The capillary temperature was maintained at 20°C and the sample tray was cooled below 5°C. An Agilent 1100 series pump equipped with a 1:100 splitter was used to deliver 5 mM ammonium acetate in 50% (v/v) methanol/water, containing 0.1 μM Hexakis to the CE interface at 10 μl/min. Here,

it was used as a sheath liquid around the outside of the CE capillary to provide a stable electrical connection between the tip of the capillary and the grounded electrospray needle. ESI-TOF-MS was conducted in negative ionization mode with the capillary voltage set to 3,500 V. For TOF-MS, the fragmentor, skimmer and Oct RF voltages were set at 100, 50 and 200 V, respectively. The flow rate of the drying nitrogen gas (heater temperature = 300°C) was 10 l/min. Automatic recalibration of each acquired spectrum was performed using reference masses of reference standards {[^{13}C isotopic ion of deprotonated acetic acid dimer (2 $CH_3COOH–H)]^-$, *m/z* 120.038339}, and {[Hexakis-deprotonated acetic acid ($CH_3COOH–H)]^-$, *m/z* 680.03554)}. Exact mass data were acquired at a rate of 1.5 spectra/s over a *m/z* range of 50–1,000.

2.8 Sample preparation for LC-TOFMS

To 30 µl of the extracellular samples, 270 µl of isopropyl alcohol containing an internal standard (2.2 µmol/l of camphor-10-sulfonic acid) was added with shaking. The mixture was centrifuged at 20,400×*g* for 10 min at 4°C, and the supernatant was then transferred to another tube and vacuum dried at 35°C. The samples were mixed with chloroform, methanol, and Milli-Q water in a volume ratio of 2:4:1 containing 20 µmol/l of 3,5-di-*tert*-butyl-4-hydroxyhydrocinnamate, centrifuged at 20,400×*g*, for 5 min at 4°C, and 25 µl of the supernatant was used for LC-TOFMS analysis.

2.9 LC-TOFMS parameters

The LC system was an Agilent 1290 infinity HPLC (Agilent Technologies). The Acquity UPLC® BEH C18 (1.7 µm), φ 2.1 × 50 mm column was purchased from Waters (Tokyo, Japan), and was maintained at 50°C. The mobile phase consisted of 0.5% acetic acid/water as eluent A and isopropanol as eluent B. A gradient of 1–99% B over 12 min was used, followed by isocratic elution at 99% for a further 17 min. The flow rate was 0.3 ml/min and the injection volume was 1 µl.

MS data were acquired on a 6530 Accurate-Mass Q-TOF LC/MS using the dual spray ESI of G-3251A (Agilent). Samples were analyzed by both positive and negative ion electrospray mass spectrometry. The MS conditions used were as follows: gas temperature 350°C, drying gas 10 l/min, nebulizer 30 psig, fragmentor 200 V, skimmer 90 V, OCT1 RF Vpp 250 V, scan range *m/z* 100–1,600 and nozzle voltage 1,000 V. The capillary voltages were 3.5 and 4.0 kV for negative and positive mode, respectively.

2.10 Determination of free amino acids

The culture medium (0.1 ml) was mixed with 0.1 ml of 10% trichloroacetic acid (Wako). After centrifugation for 5 min at 21,000×*g* at 4°C, the deproteinized supernatant was collected and stored at −30°C. The supernatants (20 µl) were analyzed using a JLC-500/V amino acid analyzer (JEOL, Tokyo, Japan) and amino acids were detected by the ninhydrin reaction (Yamazaki et al. 2007).

2.11 Data and statistical analysis

Raw data were analyzed using our proprietary software called MasterHands, which detected all possible peaks, eliminated noise and redundant features, and generated the aligned data matrix, including annotated metabolite identities and relative areas (peak areas normalized via comparison with internal standards) (Sugimoto et al. 2010b). Concentrations were calculated using external standards based on relative areas. Student's *t* test (two-tailed) was used for statistical comparisons.

3 Results and discussion

3.1 Overview of the metabolomic profiles

In total, CE-TOFMS identified 44 charged metabolites secreted by macrophages (Fig. 1; Table 1). Prostaglandin E_2 and $F_2\alpha$ were observed by LC-TOFMS as they were not charged and therefore not detected by CE-TOFMS. However, because of their similar molecular structures, these two metabolites could not be adequately resolved by LC-TOFMS, so only their combined production could be calculated and used in subsequent analyses.

3.2 Validation of the amino acid profiles determined by CE-TOFMS and the amino acid analyzer

The quantified amino acids were validated by comparing the amino acids profiles consistently obtained by CE-TOFMS with those obtained using an amino acid analyzer (Fig. 2). The metabolites present at high concentrations, such as glycine, alanine and threonine, showed slightly greater discrepancy between the profiles determined by the two methods than metabolites present at low concentrations. Nevertheless, reasonably high overall correlation coefficients were obtained for the unstimulated and LPS-stimulated macrophages, which were $R = 0.855$ ($P < 0.0001$, Pearson correlation) and $R = 0.928$ ($P < 0.0001$, Pearson correlation), respectively.

3.3 Stimulatory effect of LPS on macrophages

NO production by stimulated RAW264.7 cells was significantly increased from 0.20 to 0.66 nmol/10^6 cells/h (3.3-fold increase, $P = 0.0002$) (Fig. 3a), and TNF-α production was also significantly increased from 21.7 to 682.5 pg/10^6 cells/h

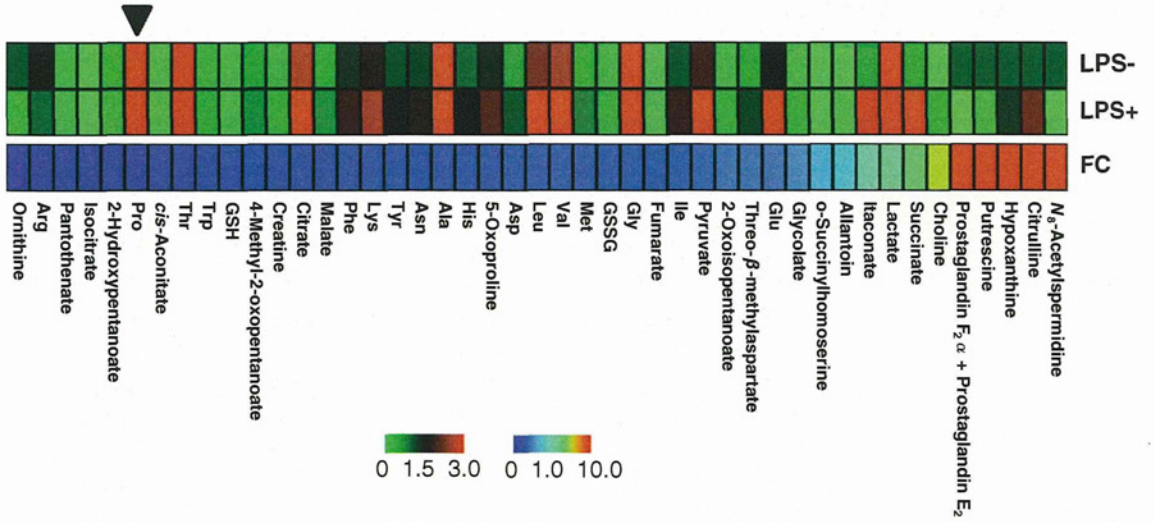

Fig. 1 *Heatmap* and *bar graph* visualization of the quantified metabolites. *Heatmap* showing the quantified metabolites using a *green–black–red scheme*, and the fold-change of metabolites in LPS+ versus LPS− cells. Where metabolites were not detected in LPS− cells, a 10-fold change was allocated. Proline, marked with *triangle*, showed no change. *FC* fold change

(31.5-fold increase, $P = 0.0151$) (Fig. 3b). Citrulline production, which accompanies NO production at a molar ratio of 1:1, is generated from arginine by inducible NO synthase (Paradise et al. 2010). It was only observed for stimulated RAW264.7 cells (2.19 nmol/10^6 cells/h, $P = 3.0 \times 10^{-5}$) (Table 1). Since NO is labile, citrulline levels are a more reliable guide to the levels of NO synthase activity. These data confirmed that LPS activated the RAW264.7 cells.

Prostaglandin E_2 and $F_2\alpha$, detected by LC-TOFMS, are central molecules in inflammatory processes. The inflammatory response of macrophages induces prostanoid synthesis by (1) inducing mobilization of the fatty acid substrate arachidonate from membrane phospholipids, (2) promoting prostaglandin H_2 production from arachidonate by upregulating cyclooxygenases 1 and 2 (COX-1/2), and (3) converting prostaglandin H_2 to specific prostanoids, such as prostaglandin E_2 and $F_2\alpha$ (Noguchi and Ishikawa 2007). The production of prostaglandin E_2 and $F_2\alpha$ (4.6×10^{-3} nmol/10^6 cells/h, $P = 1.2 \times 10^{-6}$) was only observed in stimulated RAW264.7 cells, again confirming the activation of these macrophages.

3.4 Amino acid profiles of stimulated macrophages

3.4.1 Glycine, serine and cysteine production

In amino acid profiles, glycine production was the highest of all amino acids detected (LPS− vs. LPS+: 17.1 vs. 29.5 nmol/10^6 cells/h, $P = 0.073$) (Table 1), which is consistent with previous studies using LPS-stimulated mouse macrophages and regular culture medium (DMEM + 10% FBS) (Nishiyama et al. 2010). Glycine has been reported to stimulate the production of prostaglandin E_2 and COX-2 protein in interleukin-1β-stimulated human gingival fibroblast cells, suggesting its involvement in the pathogenesis of periodontitis (Rausch-Fan et al. 2005). On the other hand, glycine has been reported to inhibit the production of inflammatory cytokines by macrophages by blocking calcium channels (Rose et al. 1999), inhibiting TNF-α secretion and increasing IL-10 production (Xu et al. 2008), or via neutral amino acid transporters (Carmans et al. 2010). Glycine inhibited the growth of an endothelial cell line (Yamashina et al. 2007) and salivary gland-derived progenitor cells (Nakamura et al. 2009). Although these data are contradictory, they mostly suggest that glycine negatively regulates the growth and activation of various cultured cells. This metabolite is also the most abundant amino acid in the saliva (Takeda et al. 2009; Tanaka et al. 2010); however, the cells in the oral cavity that secrete glycine have not been identified. In association with glycine pathway, serine, a major source of glycine, was only detected by the amino acid analyzer, but was present at relatively low concentrations (Table 1; LPS− vs. LPS+: 1.0 ± 0.074 vs. 1.1 ± 0.12 nmol/10^6 cells/h, 1.1 fold). Cysteine, which is synthesized from serine, was not observed, possibly due to the limited supply of serine.

3.4.2 Glutamate, glutamine, proline and arginine production

Glutamate, a key intermediate in amino acid metabolism, including biosynthetic and degradative pathways, is formed from α-ketoglutarate in the tricarboxylic acid (TCA) cycle. We found that glutamate production was increased by 2.2-fold ($P = 0.0043$) in activated macrophages, and its

Table 1 Profiled metabolites of RAW264.7 cells

Mode	Metabolite	LPS−		LPS+		*P* value	FC
		Mean	SD	Mean	SD		
C	Gly	17.1	7.79	29.4	4.21	0.0735	1.7
C	Ala	8.61	1.65	13.1	3.19	0.0988	1.5
C	Thr	7.50	0.594	9.13	0.501	0.0219	1.2
C	Pro	4.17	0.385	4.22	0.323	0.891	1.0
C	Val	2.50	0.424	4.18	0.361	6.41×10^{-3}	1.7
C	Leu	2.25	0.227	3.75	0.153	6.80×10^{-4}	1.7
C	Glu	1.48	0.0657	3.28	0.530	4.31×10^{-3}	2.2
C	Lys	1.72	0.231	2.54	0.337	0.0251	1.5
C	Cit	0.00	0.00	2.19	0.180	3.01×10^{-5}	N.A
C	Ile	1.04	0.232	1.86	0.0675	4.19×10^{-3}	1.8
C	Phe	1.27	0.180	1.86	0.182	0.0162	1.5
C	Asn	1.14	0.194	1.72	0.222	0.0275	1.5
C	Tyr	1.07	0.182	1.61	0.101	0.0111	1.5
C	His	0.970	0.0954	1.48	0.186	0.0134	1.5
C	Asp	0.630	0.119	1.03	0.477	0.235	1.6
C	Arg	1.62	0.196	0.958	0.0862	6.01×10^{-3}	0.59
C	Met	0.482	0.160	0.822	0.0944	0.0340	1.7
C	Trp	0.334	0.0286	0.446	0.0218	5.81×10^{-3}	1.3
C	Hypoxanthine	0.00	0.00	1.22	0.0797	1.21×10^{-5}	N.A.
C	5-Oxoproline	1.34	0.213	2.05	0.310	0.0311	1.5
C	Choline	0.0554	2.52×10^{-3}	0.408	0.0101	5.13×10^{-7}	7.4
C	Creatine	0.287	0.0418	0.401	0.0696	0.0715	1.4
C	Ornithine	1.04	0.239	0.383	0.109	0.0123	0.37
C	Putrescine	0.00	0.00	0.315	0.0605	8.36×10^{-4}	N.A.
C	Allantoin	0.0342	0.415	0.129	2.41	0.950	3.8
C	*o*-Succinylhomoserine	0.0142	0.0480	0.0475	0.0318	0.373	3.3
C	N_8-Acetylspermidine	0.00	0.00	0.0277	2.52×10^{-3}	4.55×10^{-5}	N.A.
C	GSSG	0.217	0.0323	0.371	0.0667	0.0225	1.7
C	GSH	0.118	0.0233	0.164	0.0883	0.428	1.4
A	Glycolate	0.142	0.935	0.367	0.240	0.359	2.6
A	Pyruvate	1.91	0.958	3.66	0.632	9.38×10^{-3}	1.9
A	Lactate	6.65	3.36	37.0	7.58	2.33×10^{-3}	5.6
A	Fumarate	0.0676	0.110	0.117	0.0289	0.291	1.7
A	2-Oxoisopentanoate	0.171	0.238	0.370	0.0370	0.0875	2.2
A	Succinate	0.513	0.237	3.16	0.400	3.30×10^{-4}	6.2
A	2-Hydroxypentanoate	0.379	0.198	0.328	0.0575	0.525	0.86
A	Itaconate	0.549	0.269	2.86	0.254	1.18×10^{-4}	5.2
A	4-Methyl-2-oxopentanoate	0.509	0.256	0.711	0.0391	4.20×10^{-3}	1.4
A	Malate	0.479	0.243	0.680	0.0800	0.0363	1.4
A	Threo-β-methylaspartate	0.511	0.286	1.13	0.0967	1.33×10^{-3}	2.2
A	*cis*-Aconitate	0.114	0.0579	0.123	0.0154	0.562	1.1
A	Isocitrate	0.0520	1.31	0.0444	0.0386	0.761	0.85
A	Citrate	2.62	1.32	3.69	0.485	0.0357	1.4
A	Pantothenate	0.240	0.121	0.184	0.0315	0.0818	0.77

Table 1 continued

Mode	Metabolite	LPS−		LPS+		*P* value	FC
		Mean	SD	Mean	SD		
N	Prostaglandin $F_2\alpha$+ Prostaglandin E_2	0.00	0.00	4.62×10^{-3}	1.68×10^{-4}	1.16×10^{-6}	N.A.

Units are nmol/10^6 cells/h. The metabolite concentraton in LPS− cells was 0 nmol/10^6 cells/h

SD standard deviation; *FC* fold-change; *C* cationic; *A* anionic; *N* neutral; *NA* not applicable

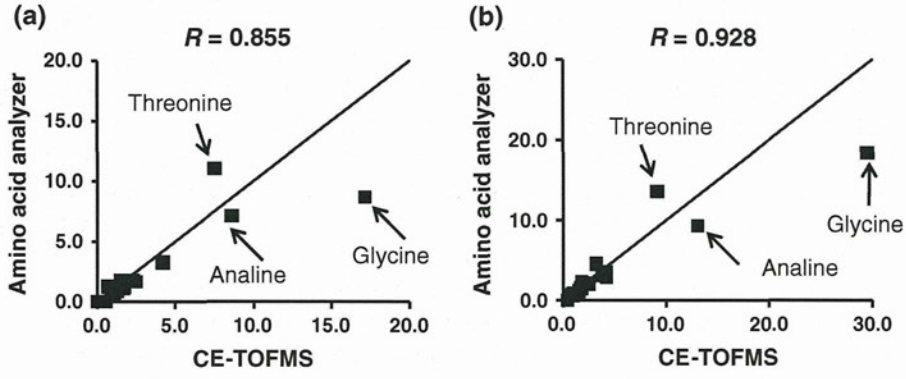

Fig. 2 Comparison of amino acid productions determined by CE-TOFMS and the amino acid analyzer for LPS− (**a**) and LPS+ macrophages (**b**). Units for both *X*- and *Y*-axis are nmol/10^6 cells/h

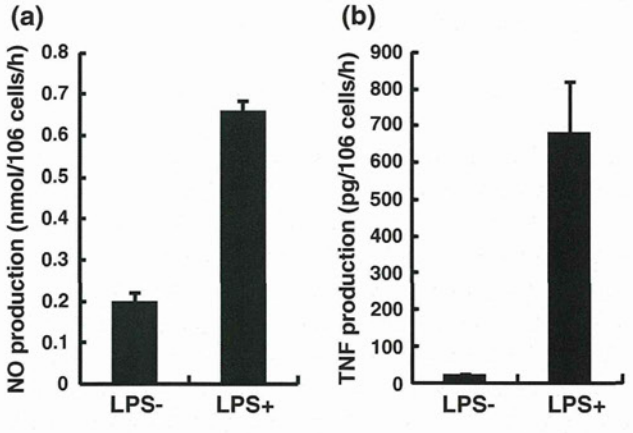

Fig. 3 Stimulation of NO (**a**) and TNF-α (**b**) production in LPS-activated RAW264.7 cells. Values are means ± standard deviation of triplicate determinations

fold-change in production was the highest observed for any amino acid. Glutamate is an excitatory neurotransmitter and the glutamate receptor protein is present on the macrophage cell surface (Noda et al. 2000). Glutamate plays a number of roles in the immune system including removal of oxidants and regulation of immune response (Li et al. 2007). Increased glutamate production in LPS-activated macrophages has already been reported (Stuckey et al. 2005). Glutamate is also a substrate in the synthesis of γ-aminobutyrate (GABA), present in macrophages (Stuckey et al. 2005). However, in this study, GABA was not detected in the culture supernatant of the activated macrophages.

Proline is synthesized from glutamate, but its concentration did not change, despite LPS stimulation (1.0-fold, $P = 0.891$). In contrast, significant decreases in arginine (0.59-fold, $P = 6.01 \times 10^{-3}$) and ornithine (0.37-fold, $P = 0.109$) were observed; ornithine is synthesized from arginine by arginase. Considering the excessive increase of citrulline upon macrophage activation, the arginine pathway seems to be highly activated and mainly used for citrulline synthesis,

3.4.3 Production of other amino acids

The production of alanine (1.5-fold, $P = 0.0988$), valine (1.7-fold, $P = 6.41 \times 10^{-3}$), and leucine (1.7-fold, $P = 6.80 \times 10^{-4}$) was increased to a similar extent by macrophage activation. The production of pyruvate, their precursor metabolite, was also elevated (1.9-fold, $P = 9.38 \times 10^{-3}$). Thus, the change of these metabolites might be due to pyruvate elevation. Aspartate (1.6-fold), which is formed from the TCA component oxaloacetate by the action of transaminase, and its downstream metabolites such as asparagine, lysine, methionine, threonine, isoleucine (from 1.2 to 1.8-fold), showed similar upregulation (Fig. 4; Table 1). On the other hand, cysteine was undetected, probably because of its degradation during sample preparation before CE-TOFMS.

3.5 Metabolomic profile of carbohydrate metabolism

3.5.1 Lactate production

Lactate production in activated macrophages was significantly elevated, and this elevation was the largest observed of all metabolites (37.0 nmol/10^6 cells/h, 5.57-fold increase, $P = 0.0023$). This finding is consistent with previous reports showing that glycolysis and lactate production were increased during osteoclast differentiation induced by receptor activator of nuclear factor [NB]-κB ligand (RANKL) in RAW264.7 cells (Kim et al. 2007). The increase in lactate production, the end product of mono-oxidative glycolysis, indicates that the glycolysis pathway is activated. Enhanced glycolysis in macrophages is likely to be a survival strategy to cope with the low oxygen conditions commonly observed at inflammatory lesions (Roiniotis et al. 2009). Lactate is a signaling molecule that can activate macrophages by stimulating inflammatory pathways, such as the TLR4 and NF-κB pathways (Samuvel et al. 2009; Nareika et al. 2005). Combined stimulation with LPS and lactate was shown to enhance macrophage activation more than LPS alone (Samuvel et al. 2009). The positive correlation between lactate production and macrophage activation observed here suggests an interaction between extracellular lactate and macrophages, possibly by a feed-forward loop, although further studies are necessary to confirm this postulation.

3.5.2 The balance between glycolysis and TCA cycle activation

Although less substantial than the change in lactate production, a significant increase in TCA cycle metabolite production was observed following macrophage activation. The levels of citrate, succinate, itaconate, malate and fumarate all increased following activation (Table 1). Rodriguez-Prados et al. (2010) observed upregulation of genes involved in glycolysis and downregulation of genes involved in the TCA cycle of LPS-activated macrophages. Indeed, the production of pyruvate in our study was significantly increased (1.9-fold, $P = 0.0094$). It is plausible that glycolysis was activated in activated macrophages under conditions where overall energy metabolism was enhanced. This implies that, even though genes in the TCA cycle were downregulated, the excessive activation of glycolysis caused a slight increase in several metabolites of the TCA cycle.

3.6 Oxidative stress

Barnes et al. (2009) found that the levels of hypoxanthine, inosine, xanthine, guanosine and guanine in gingival crevicular fluid (GCF) were elevated in inflammation sites compared with healthy sites in a human oral cavity. Their findings suggest accelerated activity of the purine degradation pathway and the production of reactive oxygen species causing marked cellular oxidative stress. In this study, we only detected hypoxanthine in activated macrophages (1.22 nmol/10^6 cells/h, $P = 1.2 \times 10^{-5}$).

GSH plays an anti-inflammatory role via its role as an antioxidant (Ghezzi 2011). The production of GSH was increased slightly (1.4-fold, $P = 0.43$), while the production of GSSG was significantly increased after activation in this study (1.7-fold, $P = 0.022$). The ratio of GSH and GSSG decreased slightly from 0.54 to 0.44 ($P = 0.64$) but this decrease was at levels below those considered significant, indicating no dramatic change in oxidative stress after treating macrophages with LPS. Allantoin, which is a uric acid oxidation product, and is therefore a marker for oxidative stress (Kand'ar et al. 2006), also showed no significant changes following exposure to LPS (3.8-fold, $P = 0.95$). These findings conflict with the elevated production of hypoxanthine, a marker for oxidative stress. Therefore, the profiling of cellular metabolites and integration of those data with the extracellular profiles determined in this study would be valuable.

3.7 Other metabolites secreted by macrophages

In addition to amino acids and metabolites related to energy metabolism, several other metabolites were also identified. The production of threo-β-methylaspartate, which is generated from oxaloacetate and NH_3 via threo-3-hydroxy-L-aspartate ammonia-lyase, was significantly increased following activation (2.2-fold, $P = 0.0013$). N_8-Acetylspermidine ($P = 4.5 \times 10^{-5}$, not detected in LPS− cells), a polyamine that generally indicates active cell growth, was only detected in activated macrophages. While the increases following activation were statistically significant ($P > 0.05$) for the following metabolites, there

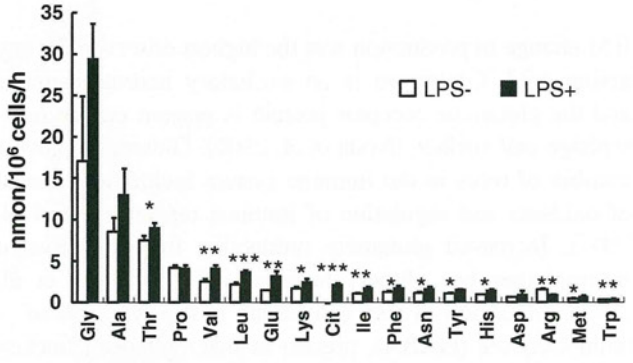

Fig. 4 *Bar graph* showing amino acid production profiles in LPS+ and LPS− cells. Values are means ± standard deviation. $*P < 0.05$, $**P < 0.01$ and $***P < 0.001$

were small increases in the production of *o*-succinylhomoserine, glyconate and 2-oxoisopentanoate, which showed high fold-changes compared with most amino acids (>1.7-fold) (Table 1). The biological relevance of these metabolites should be confirmed using other "-omics" data and cellular metabolite profiles.

4 Concluding remarks

In this study, we conducted CE-TOFMS-based metabolomics analysis to identify the metabolites secreted by LPS-stimulated macrophage-like RAW264.7 cells. Cellular activation was confirmed by the increased production of NO, citrulline, TNF-α and prostaglandins E_2 and $F_2\alpha$ by the stimulated cells. In addition to large increases in glycine production, the production of lactate was also enhanced, indicating the activation of glycolysis. Increased production of several intermediates in the TCA cycle was also observed. Of oxidative stress-related metabolites, the production of hypoxanthine was particularly high, although the GSSH/GSH ratio was almost unchanged by LPS stimulation. To understand these conflicting results, studies using integrated cellular metabolomics profiles are needed to elucidate how the observed metabolite changes contribute to the subsequent inflammatory events in periodontal disease. Nevertheless, this report provides the first catalog of the various metabolites secreted by activated macrophages, and complements prior reports on the already well-studied pro-inflammatory proteins that are known to be secreted by macrophages.

Acknowledgments This work was supported by research funds from the Yamagata Prefectural Government and the city of Tsuruoka. We thank Shinobu Abe for technical assistance.

Conflicts of interest The authors have no conflicts of interest to declare.

References

Barnes, V. M., Teles, R., Trivedi, H. M., Devizio, W., Xu, T., Mitchell, M. W., et al. (2009). Acceleration of purine degradation by periodontal diseases. *Journal of Dental Research, 88*(9), 851–855.

Bingle, L., Brown, N. J., & Lewis, C. E. (2002). The role of tumour-associated macrophages in tumour progression: Implications for new anticancer therapies. *Journal of Pathology, 196*(3), 254–265.

Carmans, S., Hendriks, J. J., Thewissen, K., Van den Eynden, J., Stinissen, P., Rigo, J. M., et al. (2010). The inhibitory neurotransmitter glycine modulates macrophage activity by activation of neutral amino acid transporters. *Journal of Neuroscience Research, 88*(11), 2420–2430.

Cronstein, B. N., Montesinos, M. C., & Weissmann, G. (1999a). Salicylates and sulfasalazine, but not glucocorticoids, inhibit leukocyte accumulation by an adenosine-dependent mechanism that is independent of inhibition of prostaglandin synthesis and p105 of NFkappaB. *Proceedings of the National Academy of Sciences of the United States of America, 96*(11), 6377–6381.

Cronstein, B. N., Montesinos, M. C., & Weissmann, G. (1999b). Sites of action for future therapy: An adenosine-dependent mechanism by which aspirin retains its antiinflammatory activity in cyclooxygenase-2 and NFkappaB knockout mice. *Osteoarthritis and Cartilage, 7*(4), 361–363.

Ghezzi, P. (2011). Role of glutathione in immunity and inflammation in the lung. *International Journal of General Medicine, 4*, 105–113.

Giannobile, W. V., Beikler, T., Kinney, J. S., Ramseier, C. A., Morelli, T., & Wong, D. T. (2009). Saliva as a diagnostic tool for periodontal disease: Current state and future directions. *Periodontology, 2000*(50), 52–64.

Kand'ar, R., Zakova, P., & Muzakova, V. (2006). Monitoring of antioxidant properties of uric acid in humans for a consideration measuring of levels of allantoin in plasma by liquid chromatography. *Clinica Chimica Acta, 365*(1–2), 249–256.

Kim, J. M., Jeong, D., Kang, H. K., Jung, S. Y., Kang, S. S., & Min, B. M. (2007). Osteoclast precursors display dynamic metabolic shifts toward accelerated glucose metabolism at an early stage of RANKL-stimulated osteoclast differentiation. *Cellular Physiology and Biochemistry, 20*(6), 935–946.

Li, P., Yin, Y. L., Li, D., Woo Kim, S., & Wu, G. (2007). Amino acids and immune function. *British Journal of Nutrition, 98*(02), 237–252.

Meyer, M. S., Joshipura, K., Giovannucci, E., & Michaud, D. S. (2008). A review of the relationship between tooth loss, periodontal disease, and cancer. *Cancer Causes and Control, 19*(9), 895–907.

Nakamura, Y., Kodama, H., Satoh, T., Adachi, K., Watanabe, S., Yokote, Y., et al. (2010). Diurnal changes in salivary amino acid concentrations. *In Vivo, 24*(6), 837–842.

Nakamura, Y., Matsumoto, S., Mochida, T., Nakamura, K., Takehana, K., & Endo, F. (2009). Glycine regulates proliferation and differentiation of salivary-gland-derived progenitor cells. *Cell and Tissue Research, 336*(2), 203–212.

Nareika, A., He, L., Game, B. A., Slate, E. H., Sanders, J. J., London, S. D., et al. (2005). Sodium lactate increases LPS-stimulated MMP and cytokine expression in U937 histiocytes by enhancing AP-1 and NF-kappaB transcriptional activities. *American Journal of Physiology—Endocrinology and Metabolism, 289*(4), E534–E542.

Nishiyama, A., Yokote, Y., & Sakagami, H. (2010). Changes in amino acid metabolism during activation of mouse macrophage-like cell lines. *In Vivo, 24*(6), 857–860.

Noda, M., Nakanishi, H., Nabekura, J., & Akaike, N. (2000). AMPA-kainate subtypes of glutamate receptor in rat cerebral microglia. *The Journal of Neuroscience, 20*(1), 251.

Noguchi, K., & Ishikawa, I. (2007). The roles of cyclooxygenase-2 and prostaglandin E_2 in periodontal disease. *Periodontology, 2000*(43), 85–101.

Paradise, W. A., Vesper, B. J., Goel, A., et al. (2010). Nitric oxide: Perspectives and emerging studies of a well known cytotoxin. *International Journal of Molecular Sciences, 11*, 2715–2745.

Pihlstrom, B. L., Michalowicz, B. S., & Johnson, N. W. (2005). Periodontal diseases. *The Lancet, 366*(9499), 1809–1820.

Ralph, P., & Nakoinz, I. (1977). Antibody-dependent killing of erythrocyte and tumor targets by macrophage-related cell lines: Enhancement by PPD and LPS. *Journal of Immunology, 119*(3), 950–954.

Rausch-Fan, X., Ulm, C., Jensen-Jarolim, E., Schedle, A., Boltz-Nitulescu, G., Rausch, W. D., et al. (2005). Interleukin-1beta-induced prostaglandin E_2 production by human gingival fibroblasts is upregulated by glycine. *Journal of Periodontology, 76*(7), 1182–1188.

Rodriguez-Prados, J. C., Traves, P. G., Cuenca, J., Rico, D., Aragones, J., Martin-Sanz, P., et al. (2010). Substrate fate in activated macrophages: A comparison between innate, classic, and alternative activation. *Journal of Immunology, 185*(1), 605–614.

Roiniotis, J., Dinh, H., Masendycz, P., Turner, A., Elsegood, C. L., Scholz, G. M., et al. (2009). Hypoxia prolongs monocyte/macrophage survival and enhanced glycolysis is associated with their maturation under aerobic conditions. *Journal of Immunology, 182*(12), 7974–7981.

Rose, M. L., Rivera, C. A., Bradford, B. U., Graves, L. M., Cattley, R. C., Schoonhoven, R., et al. (1999). Kupffer cell oxidant production is central to the mechanism of peroxisome proliferators. *Carcinogenesis, 20*(1), 27–33.

Samuvel, D. J., Sundararaj, K. P., Nareika, A., Lopes-Virella, M. F., & Huang, Y. (2009). Lactate boosts TLR4 signaling and NF-kappaB pathway-mediated gene transcription in macrophages via monocarboxylate transporters and MD-2 up-regulation. *Journal of Immunology, 182*(4), 2476–2484.

Soga, T., Baran, R., Suematsu, M., Ueno, Y., Ikeda, S., Sakurakawa, T., et al. (2006). Differential metabolomics reveals ophthalmic acid as an oxidative stress biomarker indicating hepatic glutathione consumption. *Journal of Biological Chemistry, 281*(24), 16768–16776.

Soga, T., Igarashi, K., Ito, C., Mizobuchi, K., Zimmermann, H. P., & Tomita, M. (2009). Metabolomic profiling of anionic metabolites by capillary electrophoresis mass spectrometry. *Analytical Chemistry, 81*(15), 6165–6174.

Soga, T., Ohashi, Y., Ueno, Y., Naraoka, H., Tomita, M., & Nishioka, T. (2003). Quantitative metabolome analysis using capillary electrophoresis mass spectrometry. *Journal of Proteome Research, 2*(5), 488–494.

Stuckey, D., Anthony, D., Lowe, J., Miller, J., Palm, W., Styles, P., et al. (2005). Detection of the inhibitory neurotransmitter GABA in macrophages by magnetic resonance spectroscopy. *Journal of Leukocyte Biology, 78*(2), 393.

Sugimoto, M., Goto, H., Otomo, K., Ito, M., Onuma, H., Suzuki, A., et al. (2010a). Metabolomic profiles and sensory attributes of edamame under various storage duration and temperature conditions. *Journal of Agriculture and Food Chemistry, 58*(14), 8418–8425.

Sugimoto, M., Wong, D. T., Hirayama, A., Soga, T., & Tomita, M. (2010b). Capillary electrophoresis mass spectrometry-based saliva metabolomics identified oral, breast and pancreatic cancer-specific profiles. *Metabolomics, 6*(1), 78–95.

Takahashi, J., Sekine, T., Nishishiro, M., Arai, A., Wakabayashi, H., Kurihara, T., et al. (2008). Inhibition of NO production in LPS-stimulated mouse macrophage-like cells by trihaloacetylazulene derivatives. *Anticancer Research, 28*(1A), 171–178.

Takeda, I., Stretch, C., Barnaby, P., Bhatnager, K., Rankin, K., Fu, H., et al. (2009). Understanding the human salivary metabolome. *NMR in Biomedicine, 22*(6), 577–584.

Tanaka, S., Machino, M., Akita, S., Yokote, Y., & Sakagami, H. (2010). Changes in salivary amino acid composition during aging. *In Vivo, 24*(6), 853–856.

Van Dyke, T. E., & Serhan, C. N. (2003). Resolution of inflammation: A new paradigm for the pathogenesis of periodontal diseases. *Journal of Dental Research, 82*(2), 82–90.

Xu, F. L., You, H. B., Li, X. H., Chen, X. F., Liu, Z. J., & Gong, J. P. (2008). Glycine attenuates endotoxin-induced liver injury by downregulating TLR4 signaling in Kupffer cells. *American Journal of Surgery, 196*(1), 139–148.

Yamashina, S., Ikejima, K., Rusyn, I., & Sato, N. (2007). Glycine as a potent anti-angiogenic nutrient for tumor growth. *Journal of Gastroenterology and Hepatology, 22*(Suppl 1), S62–S64.

Yamazaki, T., Yamazaki, A., Onuki, H., Hibino, Y., Yokote, Y., Sakagami, H., et al. (2007). Effect of saliva, epigallocatechin gallate and hypoxia on Cu-induced oxidation and cytotoxicity. *In Vivo, 21*(4), 603–607.

メタボロミクスによるがんの診断マーカー探索

曽　我　朋　義

メタボロミクスは，細胞や組織に存在する代謝産物の変化を，バイアスをかけない方法論で包括的に探索する手法であり，近年，幅広い研究分野に用いられるようになってきた．ここでは，疾患診断マーカー探索への応用を概説する．

メタボロミクスとは

細胞は，外界から取入れたグルコースなどの栄養源を酵素反応によってさまざまな物質に変換（代謝）し，活動するために必要な物質群を産生している．この代謝産物の総称はメタボロームとよばれ，分子量が1000以下の低分子化合物である．メタボロームの種類は生物種によって異なり，大腸菌などの微生物は数百，哺乳動物は数千，植物は数万種類が存在する．

メタボローム解析はメタボロミクスとよばれ，代謝物を大規模に測定し，代謝や細胞の働きを包括的に理解しようとする方法論である．代謝制御機構，酵素やトランスポーターの機能解明のみならず，代謝異常やがんなどの機序解明，バイオマーカー探索，疾病診断，創薬，工業用微生物の開発など，最近では幅広い分野にメタボローム解析が応

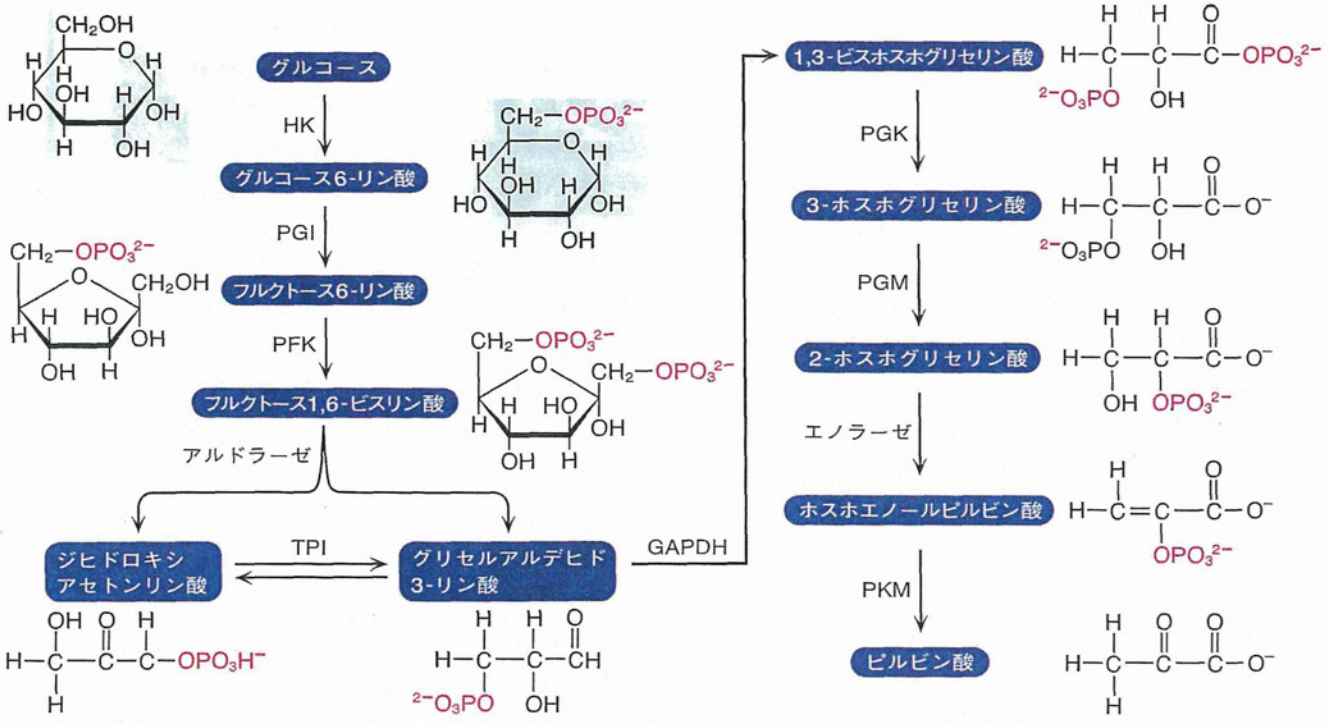

赤はリン酸基を示す．解糖系の前半の代謝物は糖にリン酸基，後半の代謝物はカルボン酸にリン酸基が結合しておりイオン性が高い．

図1　解糖系の代謝中間体の構造

用されている．

メタボローム測定の難しさ

解糖系，クエン酸回路などに代表される中心代謝の代謝中間体のほとんどは，リン酸基やカルボキシ基，アミノ基をもつイオン性化合物である（図1）．たとえば，大腸菌の場合は代謝物の約90%がイオン性化合物である．これらの代謝物の多くは，紫外吸収がなく不揮発性であり，物理的化学的性質が類似しているものから，まったく異なる性質をもつものまでが混在する．このような性質をもつ化合物群を網羅的に測定できる分析法は存在せず，さらに細胞内に数百から数万種類の代謝物が存在することが，メタボローム測定をきわめて困難にしていた．

近年いくつかのメタボローム測定法が開発された．ガスクロマトグラフィー/質量分析（GC/MS）法（文献1）は高感度，高分離能をもつ．しかし，GC/MS法によるメタボローム測定では誘導体化反応が必要であり，測定可能な代謝物は数百種類である．液体クロマトグラフィー-質量分析（LC-MS）法は（文献2）は，中性の代謝物や脂質の分析に適している．しかし，イオン性代謝物が保持されず最初に多くの物質が溶出するため，イオンサプレッション（夾雑物によってイオン化が抑制される現象）の影響を受けて定量性に乏しい．NMR法（文献3）は簡便であるが，感度が低い．どの方法も短所があり，決定的なメタボロームの測定技術は未だ開発されていない．

CE-MSによるメタボローム測定法

筆者らは，イオン性化合物に対して高い分離能を示すキャピラリー電気泳動（CE）と高感度，高選択検出器である質量分析計（MS）を組合わせたCE-MSによるメタボローム測定法を開発した（文献4）．測定原理を図2に示す．CE-MSに注入された各代謝物は，電気泳動によりキャピラリー内で分離後，質量分析計で検出される．試料中の陽イオン性物質は陰極方向に，反対に陰イオン性物質は陽極方向に，その物質の電荷/水和イオン半径の比に基づく速度で移動し，キャピラリー出口に接続された質量分析計で選択的に検出される．現在は，飛行時間型質量分析計（TOFMS）をCEに接続させたCE-TOFMS法（文献5）によって，数千種類の代謝物のいっせい分析が可能である．

がんの診断法の問題

がんを根治するためには，早期の段階でがんを発見し，全摘出することが必要である．しかし，早期のがんはほとんどが無症状であり，症状が現れた際には治療が困難な場合が多い．現在がんの診断には，腫瘍マーカーや陽電子放射断層撮影法（PET）検査（文献6）が用いられる．しかし，既存の腫瘍マーカーの多くは，化学療法や放射線療法の治療効果を判断するために開発されたものであり，がんの早期診断を目的として確立されたものではない．一方，PET検査は，がん細胞がグルコースを活発に取込む性質を利用した画像診断法であり，大腸がんなどの診断には有効な手法である．しかし，胃がん，腎がん，膀胱がん，前立腺がん，肝細胞がんなどでは診断が困難であることが知られている．現在，各種のがんを早期に発見できる診断法はほとんど存在せず，低侵襲で精度の高い各種のがんの早期診断技術が待ち望まれている．筆者らは，各種のがん患者および非がん患者から採取された血液，尿，唾液などをCE-MSメタボロミクスを用いて網羅的に測定し，腫瘍マーカーの探索を精力的に行っている．成果の一部を紹介したい．

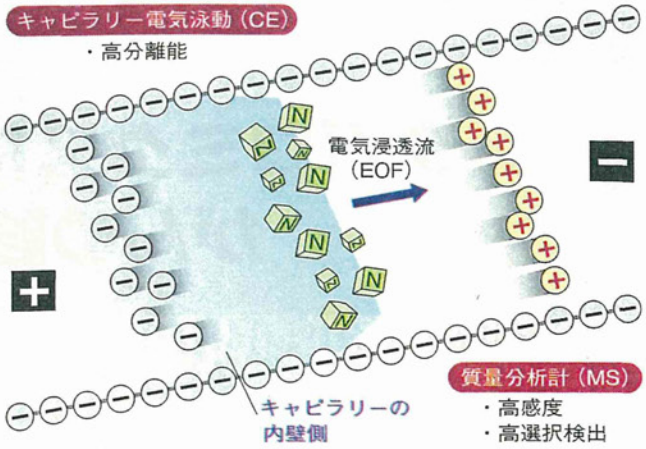

⊕，⊖，Ⓝはそれぞれ陽イオン性，陰イオン性，中性の代謝物．

図2　キャピラリー電気泳動-質量分析計（CE-MS）によるイオン性代謝物の測定方法

CE-MSメタボロミクスによる肝疾患の診断マーカー探索

肝炎ウイルスに感染した患者は，高い確率で慢性肝炎，肝硬変，肝細胞がんに進行する．肝疾患は症状もなく進行し，症状が現れたときは治療が手遅れになる場合も多く，疾患の進行度を簡便に診断できる方法が望まれている．筆者らは肝疾患の低分子診断マーカーを探索するために，山形大学医学部附属病院（試験コホート）および東京大学医学部附属病院（検証コホート）で得られた237例の各種肝疾患患者，薬剤性肝炎（DI）27例，B型肝炎持続性感染（AHB）16例，B型慢性肝炎（CHB）14例，C型肝炎持続性

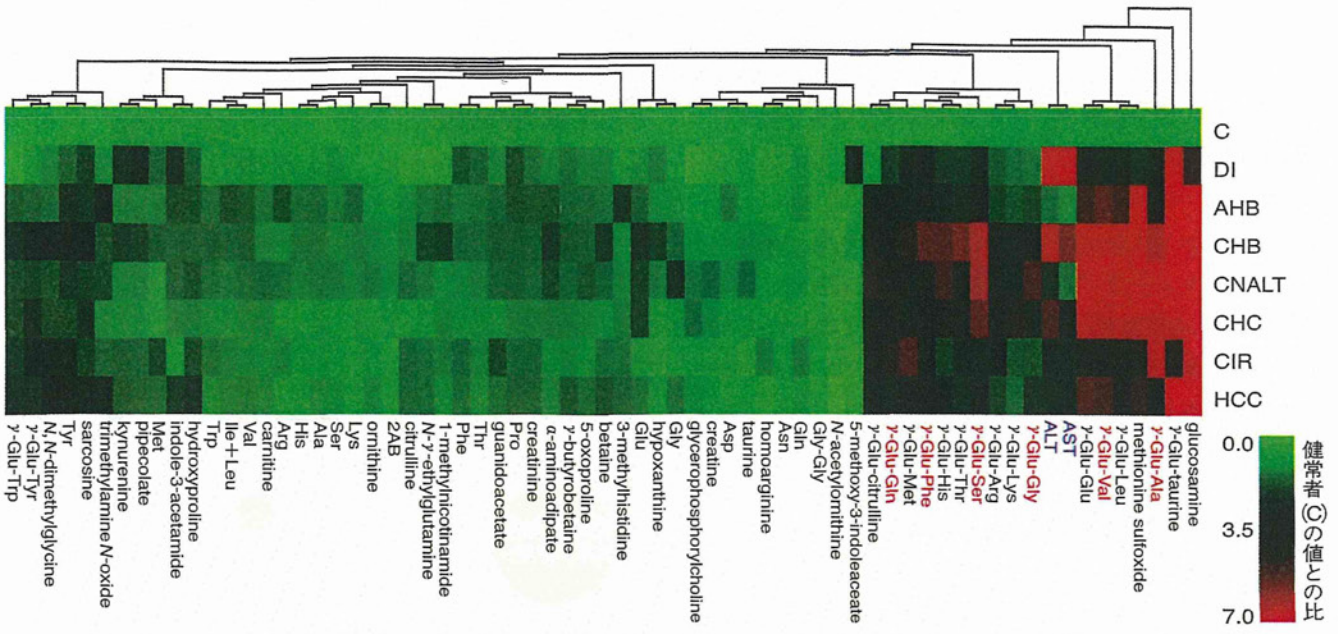

C：健常者，DI：薬剤性肝炎，AHB：B型肝炎持続性感染，CHB：B型慢性肝炎，CNALT：C型肝炎持続性感染，CHC：C型慢性肝炎，CIR：C型肝硬変，HCC：C型肝細胞がん．

図3　各肝臓疾患患者の血清中の代謝物の濃度

感染（CNALT）18例，C型慢性肝炎（CHC）35例，C型肝硬変（CIR）18例，C型肝細胞がん（HCC）32例および健常者（C）57例の血清中の代謝物をCE-TOFMSによって網羅的に測定した（文献7）．図3にヒートマップを作成したが，各種の肝疾患で十数種類のγ-グルタミルジペプチド類（γ-Glu-X；X＝アミノ酸）が高値を示した．図4に各肝疾患のAST，ALT値とγ-グルタミルジペプチド類の濃度の箱ひげ図を示した．ASTとALTは現在の肝機能マーカーだが，B型やC型肝炎持続感染では，健常者と有意な差はなかった．一方，γ-グルタミルジペプチド類の多くは，各種の肝疾患で有意に高い値を示した．

肝疾患でγ-グルタミルジペプチド類が血清中に増加す

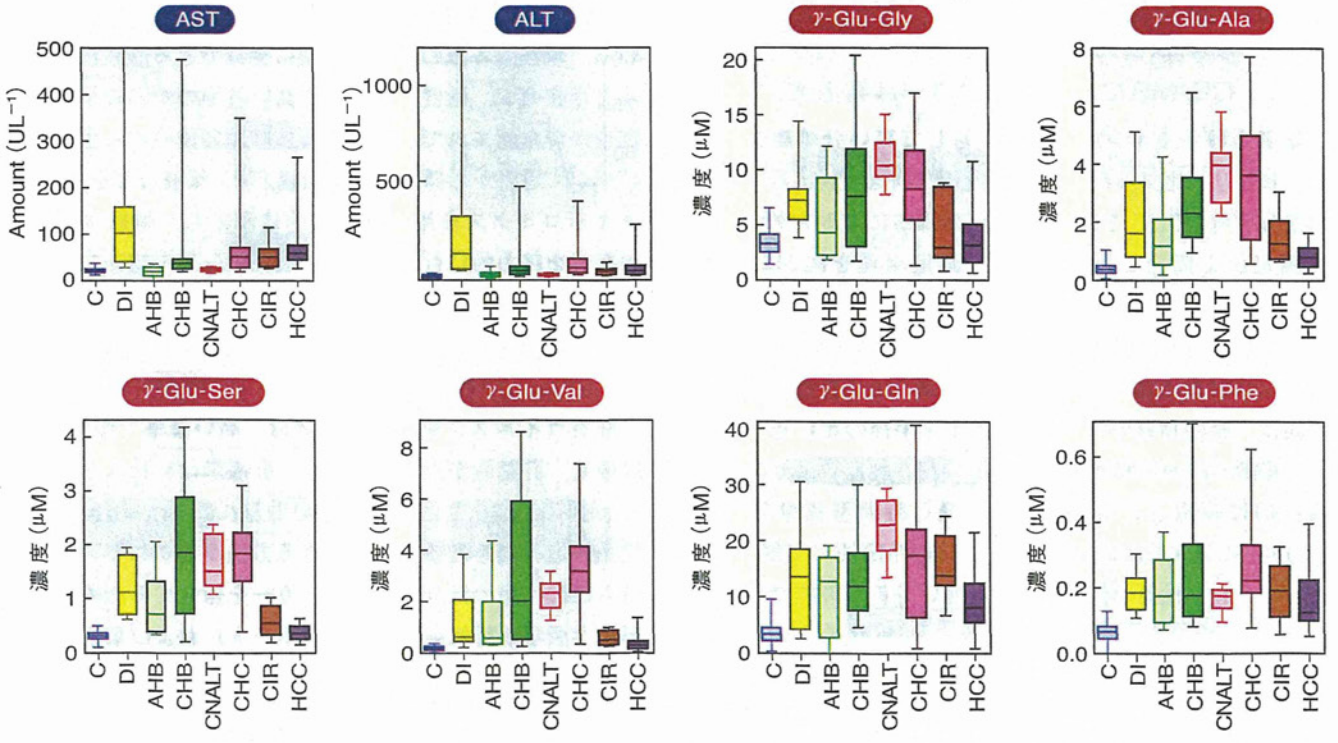

図4　各肝臓疾患患者の肝機能マーカー（AST，ALT）と血清中のγ-グルタミルジペプチド類の濃度

る機序も解明した（文献7）．もともと活性酸素種や親電子物質などの酸化ストレスが，肝疾患に深く関与していることが知られている．肝臓は酸化ストレスにさらされると，身を守るためにアミノ酸の一種システインから抗酸化物質であるグルタチオンを生合成する（図5）．筆者らは，このときに副産物としてγ-グルタミルジペプチド類が多くのアミノ酸から生合成され，血中に輸送されることを見いだしたのである（図5）．

γ-グルタミルジペプチド類による肝疾患スクリーニング

図4から，AST，ALTおよびγ-グルタミルジペプチド類は，肝疾患の種類に応じてそれぞれ特徴的な濃度で血清中に存在すること，不思議なことに，γ-グルタミルジペプチド類の種類によって肝疾患に対する変動パターンが異なることがわかった．そこで，いくつかの物質を組合わせれば各肝疾患を判別できるのではないかと考え，多変量解析の一つである多重ロジスティック回帰を用いて肝疾患を見分ける診断マーカーを探索した（図6）．診断マーカーの精度は，受信者動作特性（ROC）曲線以下の面積（AUC）で示される．たとえば，健常者を7種類の肝疾患患者から見分ける場合は，γ-Glu-Pheの値を用いるとAUCは試験コホートで0.952，検証コホートで0.967と高い精度で健常者

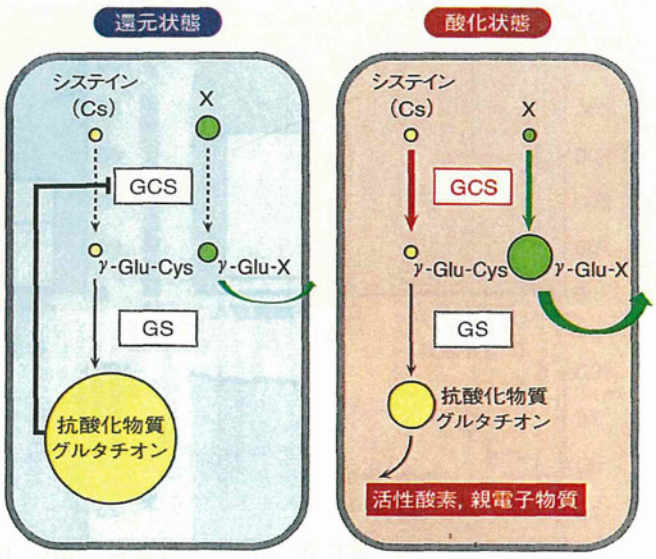

肝臓内の抗酸化物質であるグルタチオンは，システインからγ-グルタミルシステインシンセターゼ（GCS）とグルタチオンシンセターゼ（GS）によって生合成される．そのときに，多くの種類のアミノ酸やアミン（X）を基質としてGCSによってγ-グルタミルジペプチド類（γ-Glu-X）が生合成される．還元状態（健常者）では，肝臓内にグルタチオンが大量に存在するため，フィードバック制御を受けてGCSが抑制されている．しかし，酸化状態では，活性酸素や親電子物質を除去するためにグルタチオンが消費されると，GCSが活性化し，グルタチオンを生合成する．そのときにGCSによってγ-グルタミルジペプチド類が生合成され血中に輸送される．

図5　肝疾患でγ-グルタミルジペプチド類が生合成される機序

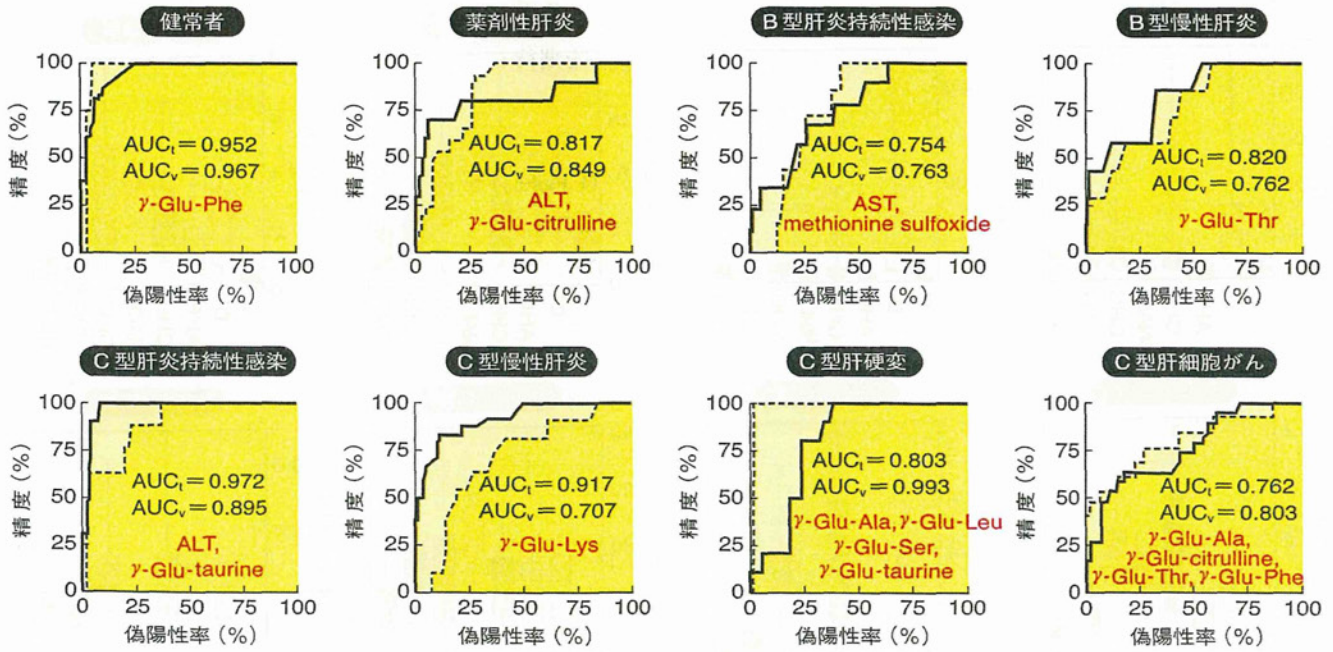

実線が試験コホート，点線が検証コホートのROC曲線．AUC_t，AUC_vは，それぞれ試験コホート，検証コホートのAUC値．グラフの中央下に色で示した代謝物をマーカーに用いて診断を行った．

図6　各肝疾患患者の受信者動作特性（ROC）曲線

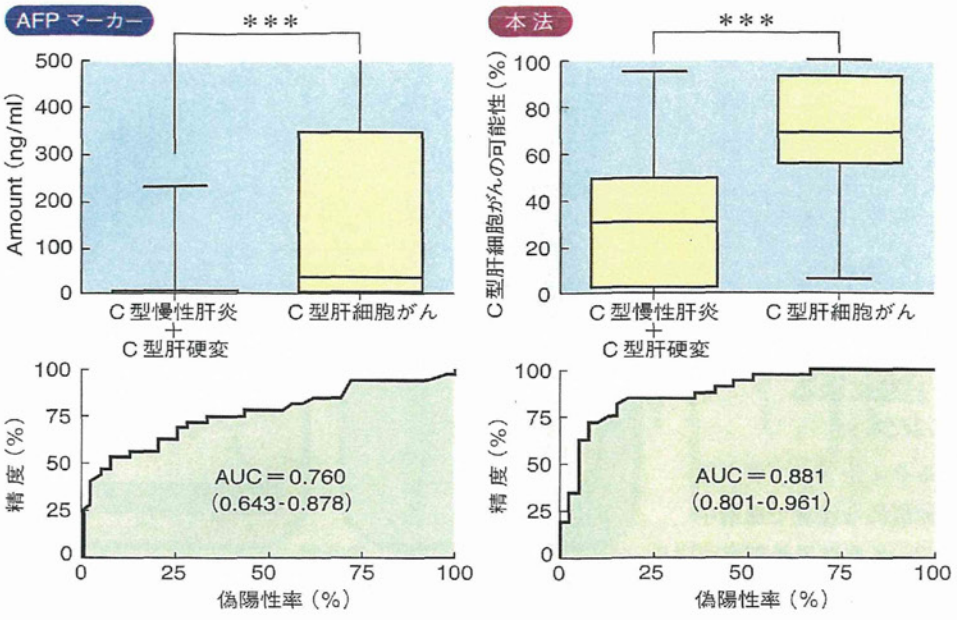

C型の慢性肝炎，肝硬変，肝細胞がん患者の中から，肝細胞がんの診断精度を既存のα-フェトプロテイン（AFP）法と比較した．

図7　肝細胞がんの診断精度の比較

を診断できることがわかった（文献7）．C型肝細胞がんをそれ以外の6種類の肝疾患および健常者から見分ける場合は，4種類のγ-グルタミルジペプチドの値を用いると試験コホートで0.762，検証コホートで0.803の精度であった．ほかの肝疾患も，いくつかを組合わせることで，高い精度でほかの疾患と区別可能であった．

さらに本法によって，C型肝細胞がん患者をC型慢性肝炎，C型肝硬変患者からどのくらいの精度で見分けることができるか，既存の肝細胞がんマーカーであるα-フェトプロテイン（AFP）と比較した（図7）．AFP法でのAUC値は0.760であったが，本法では0.881であり，本マーカーによる方法は，AFPよりも高い精度でC型肝細胞がんを慢性肝炎や肝硬変から見分けることができた（文献7）．

肝細胞がんの場合は，慢性肝炎，肝硬変，肝細胞がんと進行するため，どの段階の肝疾患か診断が可能な本法を用いれば，肝細胞がんの早期予測も可能であるだろう．筆者らは，山形県鶴岡市でメタボロームコホート研究も開始しており，本法によって肝細胞がんを早期診断することができるか検証を行う予定である．

おわりに

メタボロミクスはまだ課題も多く，有望な腫瘍マーカーとしてせっかく検出されても同定できない代謝物が半数以上存在する．未知代謝物の特定以外にも，測定精度の向上，さらなる高感度化，ハイスループット化など，やり遂げなければならない課題も多い．今後，分析化学，有機化学，合成化学，生化学などを専門とする若手の研究者がこの研究分野に参入し，メタボローム解析がさらに発展することを期待したい．

参考文献

1. O. Fiehnほか，*Nat. Biotechnol.*, 18, 1157 (2000).
2. R. Plumbほか，*Analyst*, 128, 819 (2003).
3. N. V. Reo, *Drug Chem. Toxicol.*, 25, 375 (2002).
4. T. Sogaほか，*J. Proteome Res.*, 2, 488 (2003).
5. T. Sogaほか，*J. Biol. Chem.*, 281, 16768 (2006).
6. G. J. Cookほか，*J. Clin. Oncol.*, 16, 3375 (1998).
7. T. Sogaほか，*J. Hepatol.*, 55, 896 (2011).